Deprotonation of Cationic Tungsten(IV) Aqua−Oxo−Alkyne Complexes To Form Dioxo−Vinyl Tungsten(VI) Complexes

Todd W. Crane, Peter S. White, and Joseph L. Templeton*

W. R. Kenan, Jr., Laboratory, Department of Chemistry, The University of North Carolina, Chapel Hill, North Carolina 27599-3290

Received August 18, 1999

Chiral tungsten(IV) aqua−oxo−alkyne complexes, [Tp′W(O)(H_2O)(RC≡CR)][OTf] (R = H (**1**); R = Me (**2**)); (Tp′ = hydridotris(3,5-dimethylpyrazolyl)borate; OTf = trifluoromethanesulfonate), have been prepared by halide abstraction from iodide precursors. These cationic complexes have been characterized with triflate as the counteranion. The tautomeric dihydroxo isomer has not been observed. The neutral triflate adduct Tp′W(O)(OTf)(HC≡CH) (**3**) has also been isolated. Cationic complexes **1** and **2** undergo deprotonation and isomerization when exposed to Al_2O_3 to give the dioxo−vinyl compounds Tp′W(O)$_2$(CH=CH$_2$) (**6**) and Tp′W(O)$_2$[C(Me)=C(H)(Me)] (**7**), reflecting the conversion of the W^{IV}(OH)(RC≡CR) fragment to W^{VI}(=O)(RC=CHR). The presumed intermediates, neutral oxo−hydroxo compounds Tp′W(O)(OH)(RC≡CR) (R = H (**9**); R = Me (**10**)), can be accessed by deprotonation of **1** or **2** with NaOH. Conversion of **9** to **6** was achieved thermally upon heating at 100 °C for 2 days. X-ray structural data have provided solid-state structures of both the cationic aqua complex **2** and the dioxo−vinyl complex **6**.

Introduction

Transition metal−aqua complexes are often employed as synthetic precursors because of the lability of the water ligand in many coordination compounds.[1] Recent efforts have utilized hydridotris(3,5-dimethylpyrazolyl)borate (Tp′) type ligands to improve the air and thermal stability of aqua complexes of ruthenium.[2−4] Despite the lability of the water, attempts to perform catalytic couplings[5] and ring-closing metathesis reactions[6] with these [TpL$_2$Ru−OH$_2$]$^+$ precursors have been unsuccessful.

An important feature of metal−aqua complexes is their relationship to metal hydroxo[7,8] and oxo compounds.[9−11] Recent work by Moro-oka and co-workers reported structures of monomeric and dimeric hydroxo complexes and described their ability to eliminate water upon the addition of ROOH to form hydroperoxo and alkylperoxo structures.[12,13] Such complexes are postulated as key catalytic oxygenation intermediates involved in organic and metabolic transformations. Related work by Young and co-workers involves the modeling of molybdoenzymes containing the [$Mo^{VI}O_2$]$^{2+}$ active site using Tp′Mo(O)$_2$(SPh) (Tp′ = hydridotris(3,5-dimethylpyrazolyl)borate). Along with the Mo(VI) dioxo species, the Mo(V) oxo−hydroxo complex, Tp′Mo(O)(OH)(SPh), and the Mo(IV) oxo−aqua adduct, Tp′Mo(O)(H_2O)(SPh), were generated.[14−17]

Tungsten and molybdenum complexes that contain both oxo and alkyne moieties within the same coordination sphere have been known for over 2 decades.[18−23] These M(IV) (M = Mo, W) d^2 compounds provide an interesting contrast to the more extensive series of M(II), d^4 carbonyl−alkyne compounds that have also been characterized.[24−31] The former complexes pair

(1) Beck, W.; Sunkel, K. *Chem. Rev.* **1988**, *88*, 1405.
(2) Takahashi, Y.; Akita, M.; Hikichi, S.; Moro-oka, Y. *Inorg. Chem.* **1998**, *37*, 3186.
(3) Tenorio, M. A. J.; Tenorio, M. J.; Puerta, M. C.; Valerga, P. *J. Chem. Soc., Dalton Trans.* **1998**, *21*, 3601.
(4) Trimmel, G.; Slugovc, C.; Wiede, P.; Mereiter, K.; Sapunov, V. N.; Schmid, R.; Kirchner, K. *Inorg. Chem.* **1997**, *36*, 1076.
(5) Gemel, C.; Trimmel, G.; Slogovc, C.; Kremel, S.; Mereiter, K.; Schmid, R.; Kirchner, K. *Organometallics* **1996**, *15*, 3998.
(6) Sanford, M. S.; Henling, L. M.; Grubbs, R. H. *Organometallics* **1998**, *17*, 5384.
(7) Gilje, J. W.; Roesky, H. W. *Chem. Rev.* **1994**, *94*, 895.
(8) Bryndza, H. E.; Tam, W. *Chem. Rev.* **1988**, *88*, 1163.
(9) Nugent, W. A.; Mayer, J. M. *Metal Ligand Multiple Bonds*; Wiley: New York, 1988.
(10) Che, C.-M.; Yam, V. W.-W. *Adv. Inorg. Chem.* **1992**, *39*, 233.
(11) Griffith, W. P. *Chem. Soc. Rev.* **1992**, 179.
(12) Akita, M.; Miyaji, T.; Hikichi, S.; Moro-oka, Y. *Chem. Commun.* **1998**, 1005.
(13) Hikichi, S.; Komatsuzaki, H.; Kitajima, N.; Akita, M.; Mukai, M.; Kitagawa, T.; Moro-oka, Y. *Inorg. Chem.* **1997**, *36*, 266.
(14) Xiao, Z.; Young, C. G.; Enemark, J. H.; Wedd, A. G. *J. Am. Chem. Soc.* **1992**, *114*, 9194.
(15) Xiao, Z.; Bruck, M. A.; Enemark, J. H.; Young, C. G.; Wedd, A. G. *Inorg. Chem.* **1996**, *35*, 7508.
(16) Xiao, Z.; Bruck, M. A.; Doyle, C.; Enemark, J. H.; Grittini, C.; Gable, R. W.; Wedd, A. G.; Young, C. G. *Inorg. Chem.* **1995**, *34*, 5950.
(17) Xiao, X.; Gable, R. W.; Wedd, A. G.; Young, C. G. *J. Am. Chem. Soc.* **1996**, *118*, 2912.
(18) Bokiy, N. G.; Gatilov, Y. V.; Struchkov, Y. T.; Ustynyuk, N. A. *J. Organomet. Chem.* **1973**, *54*, 213.
(19) Howard, J. A. K.; Stansfield, R. F. D.; Woodward, P. *J. Chem. Soc., Dalton Trans.* **1976**, 246.
(20) Maatta, E. A.; Wentworth, R. A. D. *Inorg. Chem.* **1979**, *18*, 524.
(21) Maatta, E. A.; Wentworth, R. A. D.; Newton, W. E.; McDonald, J. W.; Watt, G. D. *J. Am. Chem. Soc.* **1978**, *100*, 1320.
(22) Newton, W. E.; McDonald, J. W.; Corbin, J. L.; Ricard, L.; Weiss, R. *Inorg. Chem.* **1980**, *19*, 1997.
(23) Templeton, J. L.; Ward, B. C.; Chen, G. J.-J.; McDonald, J. W.; Newton, W. E. *Inorg. Chem.* **1981**, *20*, 1248.
(24) Templeton, J. L. *Adv. Organomet. Chem.* **1989**, *29*, 1.
(25) Winston, P. B.; Burgmayer, S. J. N.; Templeton, J. L. *Organometallics* **1983**, *2*, 167.
(26) Winston, P. B.; Burgmayer, S. J. N.; Tonker, T. L.; Templeton, J. L. *Organometallics* **1986**, *5*, 1707.
(27) Feng, S. G.; Phillipp, C. C.; Gamble, A. S.; White, P. S.; Templeton, J. L. *Organometallics* **1991**, *10*, 3504.
(28) McDonald, J. W.; Corbin, J. L.; Newton, W. E. *J. Am. Chem. Soc.* **1975**, *97*, 1970.
(29) McDonald, J. W.; Newton, W. E.; Creedy, C. T. C.; Corbin, J. L. *J. Organomet. Chem.* **1975**, *92*, C25.
(30) Richard, L.; Weiss, R.; Newton, W. E.; Chen, G. J.-J.; McDonald, J. W. *J. Am. Chem. Soc.* **1978**, *100*, 1318.

10.1021/ic990994y CCC: $19.00
Published on Web 02/25/2000

Scheme 1. Qualitative MO Diagrams for Alkyne Orientation

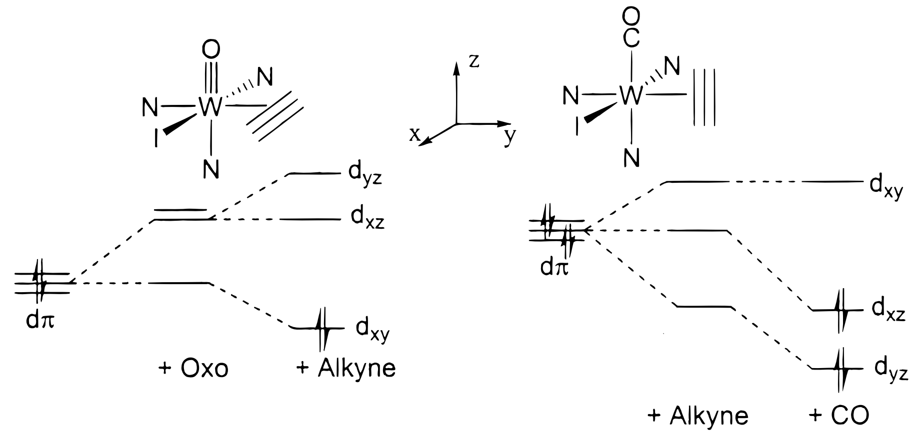

Scheme 2. Elaborations of W(II) and W(IV) Alkynes

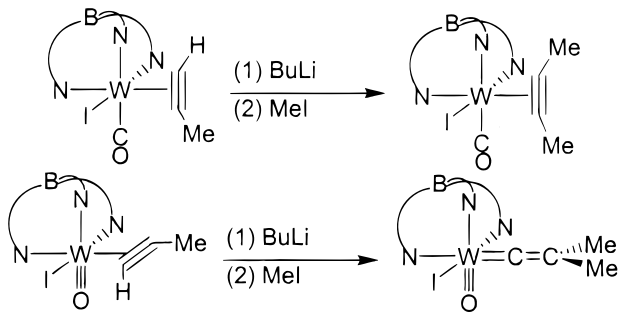

the π-basic oxo unit with the amphoteric alkyne ligand, while the latter compounds combine the quintessential π-acid, carbon monoxide, with the alkyne fragment. In the oxo−alkyne case, donation from one oxygen p orbital into a metal d orbital forms a two-center−two-electron bond. Competition between the second filled oxygen p orbital and the filled alkyne $\pi_\perp$ orbital for the same vacant metal dπ orbital produces a three-center−four-electron bond. In the carbonyl−alkyne system, stabilization occurs because of back-donation from two metal d orbitals to the π^* orbitals of the CO ligand. Bonding in both systems is completed by back-donation from a filled metal dπ orbital to the vacant alkyne $\pi_{\|}^*$, in the CO case as a three-center−two-electron π bond. Scheme 1 shows how the bonding interactions among the metal dπ orbitals and the ligand p and π orbitals combine to accommodate these d^2 and d^4 configurations within an octahedral environment. In accord with the change in oxidation state, the key geometrical difference between the two compounds is a 90° rotation of the alkyne C≡C vector with respect to L (L = O or CO).

Recent work indicates that the difference in alkyne orientation is important when comparing the chemistry of d^4 alkyne systems to that of the d^2 oxo−alkyne compounds. For instance, elaboration of Tp′W(CO)(HC≡CMe)(I) via deprotonation of the terminal alkyne site followed by methylation generated the 2-butyne complex.[32] In contrast, when the same sequence is applied to Tp′W(O)(HC≡CMe)(I), the C_2 fragment rearranges to give a tungsten−dimethylvinylidene as the final product (Scheme 2).[33] The present study extends the chemistry of the Tp′W(O)(alkyne) fragment to cationic oxo−alkyne systems, namely, the aqua complexes [Tp′W(O)(H_2O)(RC≡CR)][OTf] (OTf = trifluoromethanesulfonate).

Results and Discussion

Synthesis of [Tp′W(O)(H_2O)(RC≡CR)][OTf] (R = H (1); R = Me (2)), Tp′W(O)(OTf)(HC≡CH) (3), and [Tp′W(O)(H_2O)(MeC≡CH)][OTf] (4). Addition of AgOTf to a yellow methylene chloride solution containing Tp′W(O)(I)(HC≡CH) and excess water resulted in the immediate formation of AgI precipitate. Continued stirring for 2.5 h and removal of AgI via filtration through Celite resulted in a pale-yellow solution. The ^{1}H NMR of the crude yellow solid, which was isolated by precipitation with pentane, revealed evidence for a complex with coordinated water and a second minor chiral species, the neutral triflate adduct Tp′W(O)(OTf)(HC≡CH) (**3**), present in a 4:1 ratio. Recrystallization of the solid from CH_2Cl_2/pentanes produced yellow needles that were washed with a cold 1:1 mixture of the recrystallizing solvents to obtain the clean water complex [Tp′W(O)(H_2O)(HC≡CH)][OTf] (**1**) (eq 1). Diffraction

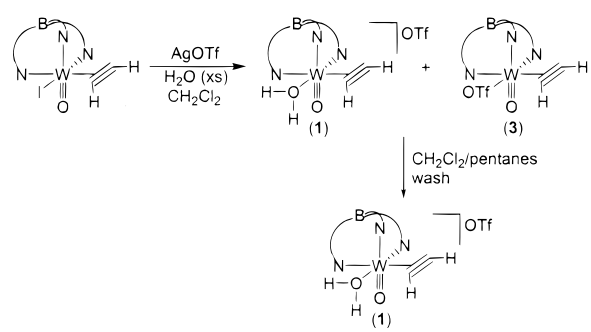

(1)

data for **1** were collected, but refinement of the structure proved difficult because of the presence of disorder among independent molecules in the unit cell. Following the same procedure, the analogous 2-butyne complex, [Tp′W(O)(H_2O)(MeC≡CMe)]-[OTf] (**2**), was synthesized. X-ray quality crystals of **2** were obtained to provide a solid-state structure of an aqua−oxo tungsten−alkyne complex (vida infra).

Dissolving the yellow crystals of **1** in CD_2Cl_2 showed that the chiral water complex has the expected six distinct singlets in the methyl region for the pyrazolyl methyl groups and three singlets for the pyrazolyl ring protons of Tp′ in the ^{1}H NMR. The inequivalence of the pyrazole groups indicates that proton transfer between the oxo and aqua ligands is slow on the NMR time scale. Three informative ^{1}H NMR signals appear above 10 ppm. The coordinated acetylene protons appear as singlets at 12.01 and 10.63 ppm, both with $^2J_{WH}$ = 15 Hz (^{183}W, 14%;

(31) Ward, B. C.; Templeton, J. L. *J. Am. Chem. Soc.* **1980**, *102*, 1532.
(32) Wells, M. B.; White, P. S.; Templeton, J. L. *Organometallics* **1997**, *16*, 1857.
(33) Crane, T. W.; White, P. S.; Templeton, J. L. *Organometallics* **1999**, *18*, 1897.

$I = 1/2$). This 1.4 ppm chemical shift difference is likely due to the ring current effects of Tp′.[26,33] In accord with previous correlations, the signal at 12.01 ppm is attributed to the acetylene proton anti to the Tp′ pyrazolyl ring while the resonance at 10.63 ppm is assigned to the acetylene proton syn to Tp′. Perhaps most unique for this complex is a broad singlet at 10.05 ppm that integrates cleanly for two hydrogens and is assigned to the coordinated water molecule.

Attempts to displace the water ligand via the addition of an excess of CH_3CN (ca. 6 equiv) to an NMR sample of **1** resulted in a 8:2.5:1 ratio of water complex **1** to triflate complex **3** to putative nitrile adduct $[Tp'W(O)(CH_3CN)(HC{\equiv}CH)]^+$. After 24 h, this ratio had only changed to 3:1:1 (9:3:3), suggesting that nitrile displacement of water is relatively slow.[6] Addition of excess water (ca. 3 equiv) to an NMR sample of chiral water complex **1** initiated a dynamic process that resulted in a ^{1}H NMR spectrum involving a complex of effective C_s symmetry. In particular, two of the three pyrazole proton signals and four of the six Tp′ methyl resonances were significantly broadened. Sharp Tp′ signals reminiscent of the room-temperature spectrum in the absence of water and indicative of a chiral complex were evident in low-temperature ^{1}H NMR experiments. Conversely, both acetylene resonances are sharp at room temperature in the ^{1}H NMR spectrum even in the presence of added water. Upon cooling of the sample, the acetylene resonance at 10.6 ppm remains sharp while the acetylene signal near 11.8 ppm becomes broad. Possible origins for these dynamic processes will be discussed below.

The acetylene carbons of water complex **1** are found at 156.8 and 148.2 ppm in the ^{13}C NMR spectrum, with similar $^1J_{WC}$ values of 28 and 30 Hz, respectively. These shifts are nearly identical to those found for the alkyne carbons in the neutral $Tp'W(O)(I)(HC{\equiv}CH)$ complex (156.8 and 145.3 ppm, both with $^1J_{WC} = 30$ Hz), indicating that the alkyne serves as a formal three-electron donor in both the neutral and cationic complexes.[33]

The ^{13}C NMR spectrum for **1** also shows a quartet centered at 120.1 ppm with $^1J_{CF} = 318$ Hz for the CF_3 group of the triflate counteranion. Evidence for triflate serving as the counteranion is found in the solid-state IR where a stretch at 1293 cm^{-1} is assigned to the SO_3 group.[34,35] Additional IR data for **1** include the W═O stretch at 960 cm^{-1} and a broad O−H stretch near 3100 cm^{-1} for the coordinated water molecule.

Synthesis of the aqua−propyne complex $[Tp'W(O)(H_2O)(MeC{\equiv}CH)]^+$ (**4**) led to two isomers. When starting with a single alkyne rotamer of the iodide−propyne precursor $Tp'W(O)(MeC{\equiv}CH)(I)$, addition of AgOTf and an excess of water resulted in the formation of two products. The ^{1}H NMR of this mixture displayed two sets of Tp′ and alkyne signals in about a 4:1 ratio. The major product, *syn*-$[Tp'W(O)(H_2O)(MeC{\equiv}CH)]^+$ (*syn*-**4**), has the alkyne methyl group pointed toward the Tp′ pyrazole ring as indicated by the downfield chemical shift for the terminal propyne resonance at 11.90 ppm in the ^{1}H NMR. The minor product, *anti*-**4**, displays the alkyne terminal proton signal at 10.60 ppm, suggesting that the propyne methyl group is aligned next to the water ligand (eq 2). Both terminal signals

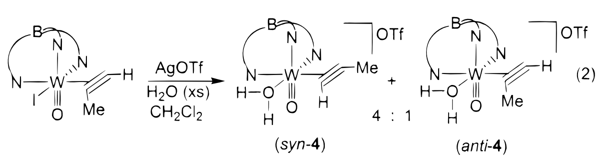

(34) Lawrance, G. A. *Chem. Rev.* **1986**, *86*, 17.
(35) Johnston, D. H.; Shriver, D. F. *Inorg. Chem.* **1993**, *32*, 1045.

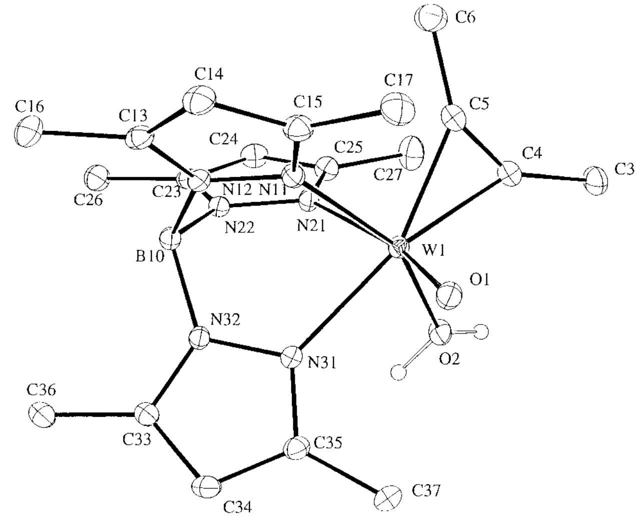

Figure 1. ORTEP diagram of $Tp'W(O)(H_2O)(MeCCMe)^+$ (**2**).

Table 1. Selected Bond Distances (Å) and Bond Angles (deg) for $[Tp'W(O)(H_2O)(MeC{\equiv}CMe)][OTf]$ (**2**)

W(1)−O(1)	1.708(2)	W(1)−N(11)	2.178(2)
W(1)−O(2)	2.094(2)	W(1)−N(21)	2.292(2)
W(1)−C(4)	2.090(3)	W(1)−N(31)	2.226(2)
W(1)−C(5)	2.090(3)	C(3)−C(4)	1.492(5)
C(4)−C(5)	1.278(5)	C(5)−C(6)	1.480(5)
O(2)−O(42)[a]	2.660(3)	O(2)−O(43)[a]	2.639(3)
O(1)−W(1)−O(2)	102.89(9)	C(4)−W(1)−N(21)	94.59(11)
O(1)−W(1)−C(4)	98.12(11)	C(4)−W(1)−N(21)	160.75(11)
O(1)−W(1)−C(5)	104.78(11)	O(2)−W(1)−C(5)	114.68(10)
O(1)−W(1)−N(11)	89.30(10)	O(2)−W(1)−N(11)	155.30(9)
O(1)−W(1)−N(21)	166.73(9)	O(2)−W(1)−N(21)	82.39(9)
O(1)−W(1)−N(31)	88.28(10)	O(2)−W(1)−N(31)	78.01(9)
O(2)−W(1)−C(4)	82.86(11)	C(5)−W(1)−N(11)	81.92(11)
C(4)−W(1)−N(11)	117.01(11)	C(5)−W(1)−N(21)	83.51(11)

[a] O(42) and O(43) belong to the bridging OTf groups seen in the solid-state dimeric structure of **2** (Figure 2).

also display coupling to the alkyne methyl group with $^4J_{HH} = 3$ Hz and $^2J_{WH} = 14$ Hz. The origin of this alkyne rotation during ligand substitution will be considered below (vide infra).

The minor product formed during the synthesis of **1** is the neutral triflate adduct $Tp'W(O)(OTf)(HC{\equiv}CH)$ (**3**). This complex can be generated in good yield by adding fresh AgOTf to $Tp'W(O)(I)(HC{\equiv}CH)$ in dry methylene chloride. The ^{1}H NMR spectrum of **3** shows the acetylene proton resonances at 12.47 and 10.71 ppm, each with $^2J_{WH}$ of 15 Hz. The acetylene carbons are found at 156.5 and 148.6 ppm ($^1J_{WC} = 29$ Hz), and the quartet for the CF_3 group of the coordinated triflate appears at 119.3 ppm in the ^{13}C NMR spectrum. The IR spectrum for **3** includes the W═O stretch at 986 cm^{-1}, and a band at 1335 cm^{-1} attributed to the SO_3 group of the coordinated triflate.[34]

X-ray Structure of $[Tp'W(O)(H_2O)(MeC{\equiv}CMe)][OTf]$ (2). An ORTEP diagram of cationic aqua complex **2** with the triflate counteranion omitted is shown in Figure 1. Selected bond distances and angles are given in Table 1. The most salient geometrical features are the W═O distance, 1.708(2) Å, which lies within the typical range of other monomeric tungsten−oxo compounds,[9] and the W−OH_2 separation of 2.094(2) Å, which is similar to that observed in a tungsten(IV)−water complex reported by Green et al. (2.084 Å)[38] but somewhat shorter than

(36) Mayer, J. M.; Tulip, T. H.; Calabrese, J. C.; Valencia, E. *J. Am. Chem. Soc.* **1987**, *109*, 157.
(37) Cundari, T. R.; Conry, R. R.; Spaltenstein, E.; Critchlow, S. C.; Hall, K. A.; Tahmassebi, S. K.; Mayer, J. M. *Organometallics* **1994**, *13*, 322.

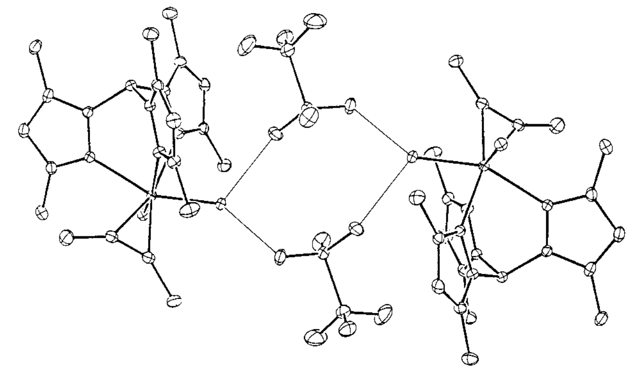

Figure 2. ORTEP diagram of (**2**) showing bridging OTf groups.

that observed for the W(0) complex $W(CO)_3(PR_3)_2(H_2O)$ (2.320 Å).[39] The large 0.37 Å difference between the W−OH_2 and W═O bond lengths clearly distinguishes these fragments from one another. The two W−C(alkyne) distances are identical at 2.090(3) Å and fit into the range characteristic of tungsten−alkyne systems where the alkyne serves as a formal three-electron donor.[24] The three W−N bond lengths of 2.2922(25), 2.2263(25), and 2.1779(24) Å reflect the decreasing trans influence of oxo, alkyne, and water ligands, respectively. Figure 2 shows that the complex actually has a structure in the solid state arising from two triflate anions serving to link the cations in pairs. The O(2)···O(42) and O(2)···O(43) separations of 2.660(3) and 2.639(3) Å indicate the presence of hydrogen bonding between the water hydrogens and the bridging triflate oxygens. The distances and hydrogen bonding in the dimeric structure of **2** are similar to results reported for [TpRu(L)-(H_2O)][OTf] (L = COD, $Ph_2PCH_2CH_2NMe_2$).[4,5]

Synthesis and Characterization of Tp′W(O)$_2$(CH═CH$_2$) (6), Tp′W(O)$_2$[CMe═C(H)(Me)] (7), and Tp′W(O)$_2$(CMe═CH$_2$) (8). Initial attempts to separate mixtures containing both the aqua complex **1** and the triflate complex **3** using chromatography on alumina failed. The green-yellow mixture was loaded on the column with CH_2Cl_2 and eluted with increasing CH_2Cl_2/hexanes ratios. The column required analysis using thin-layer chromatography (TLC) because no colored fractions moved with the eluting solvents. A single product, neither **1** nor **3**, was observed by TLC in most cases, but on a few occasions a second minor product was detected. To obtain the highest minor to major product ratio, a short plug of alumina was used with 100% CH_2Cl_2 as the eluting solvent.

The major product did not display signals in the region of the ^{1}H NMR indicative of coordinated acetylene. The Tp′*H* and Tp′CH_3 regions displayed signals with a 1:2 ratio, indicating the presence of a mirror plane of symmetry. Most informative was a set of three proton signals matching a vinyl fingerprint, XCH═CH_2; three sets of doublets of doublets between 6 and 8 ppm indicated the presence of a tungsten−vinyl fragment. The presence of a mirror plane of symmetry and resonances symptomatic of a vinyl fragment implicated a dioxo−vinyl complex, Tp′W(O)$_2$(CH═CH$_2$) (**6**), as the likely structure (eq 3). This

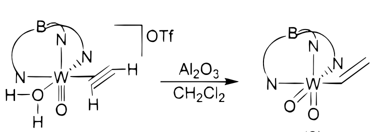

(**6**) (3)

formulation was confirmed by X-ray diffraction (vide infra). In contrast, the ^{1}H NMR of the minor product, **9**, displayed a new set of coordinated acetylene signals and distinct chemical shifts for each of the Tp′*H* and Tp′CH_3 resonances, implying a new chiral oxo−alkyne complex (vide infra).

In the ^{1}H NMR of **6**, the doublet of doublets furthest downfield is centered at 7.46 ppm and assigned as the lone hydrogen on C_α. The larger splitting of 19.3 Hz is assigned to $^3J_{HH}$(trans), while the smaller 13.6 Hz coupling is a reasonable $^3J_{HH}$(cis) value. Each peak in this four-line pattern also displays two-bond coupling to tungsten of 4.8 Hz. The set of doublets centered at 6.98 ppm in the ^{1}H NMR spectrum has $^3J_{HH} = 13.6$ Hz, $^2J_{HH} = 3.2$ Hz, and $^3J_{WH} = 16.0$ Hz. This pattern is assigned to the proton on C_β that is cis to the C_α proton. The trans hydrogen is centered at 6.14 ppm and has the corresponding $^3J_{HH}$ and $^2J_{HH}$ values of 19.3 and 3.2 Hz, respectively, with $^3J_{WH} = 8.7$ Hz. The ^{13}C resonances for the vinyl fragment appear at 177.7 ppm (C_α) and 135.8 ppm (C_β). Tungsten coupling to both vinyl carbons is observed with values of $^1J_{WC} = 151$ Hz and $^2J_{WC} = 29$ Hz. The magnitude of the one-bond tungsten coupling is comparable to values for carbonyl and carbene ligands with multiple bond character. Additionally, the IR spectrum of **6** has typical symmetric and antisymmetric W═O frequencies of 945 and 905 cm^{-1}, respectively. Analytical results indicated that a molecule of methylene chloride, observed in the solid-state X-ray structure, should be factored into the weight percent calculations. A tungsten(VI) vinyl complex, Tp′W(O)$_2$(CH═CMe$_2$), has been reported by Sundermeyer and co-workers.[40]

The related complexes, Tp′W(O)$_2$[C(Me)═C(H)(Me)] (**7**) and Tp′W(O)$_2$(CMe═CH$_2$) (**8**), were synthesized in a fashion similar to **6** by starting with [Tp′W(O)(H_2O)(MeC≡CMe)][OTf] (**2**) and [Tp′W(O)(H_2O)(MeC≡CH)][OTf] (**4**), respectively. Dioxo−vinyl **7** was obtained as a mixture of two isomers that could be distinguished by low-temperature NMR. At −50 °C, the ^{1}H NMR spectrum showed two vinyl complexes in a ratio of 10:1 each displaying the expected 2:1 patterns for the Tp′ resonances. The proton attached to C_β appears at 5.10 ppm as a quartet with $^3J_{HH} = 6$ Hz, while the methyl attached to C_β is a 6 Hz doublet at 1.28 ppm for the major isomer. The quartet and doublet of the C_β vinyl site for the minor isomer are centered at 6.74 and 1.55 ppm, respectively. We believe the isomers reflect a barrier to rotation around the W−C vinyl bond (eq 4).

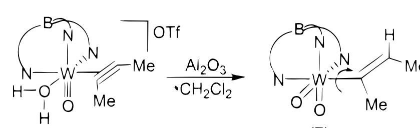

(**7**) (4)

Although cis and trans isomers are possible for the vinyl ligand, the associated rotational barrier would presumably be too high for the isomer interconversion rate observed here.

While the aqua−propyne complex **4** is isolated as a 4:1 mixture of alkyne rotamers, subsequent reaction with Al_2O_3 gave a single dioxo−vinyl product **8** (eq 5). The protons attached to

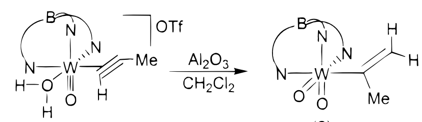

(**8**) (5)

C_β appear as broad singlets at 6.24 and 4.71 ppm. The former

(38) Green, M. L. H.; Parkin, G.; Chen, M.; Prout, K. *J. Chem. Soc., Dalton Trans.* **1986**, 2227.
(39) Kubas, G. J.; Burns, C. J.; Khalsa, G. R. K.; Van Der Sluys, L. S.; Kiss, G.; Hoff, C. D. *Organometallics* **1992**, *11*, 3390.
(40) Adam, W.; Putterlik, J.; Schuhmann, R. M.; Sundermeyer, J. *Organometallics* **1996**, *15*, 4586.

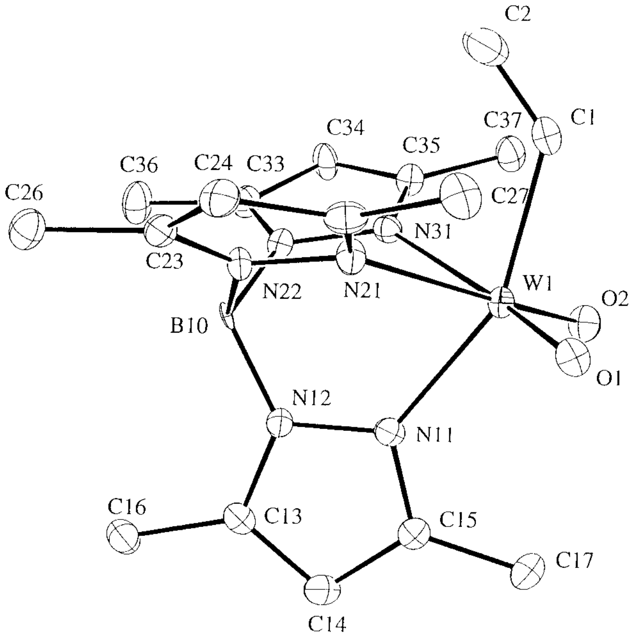

Figure 3. ORTEP diagram of Tp′W(O)$_2$(CH=CH) (**6**).

Table 2. Selected Bond Distances (Å) and Bond Angles (deg) for Tp′W(O)$_2$(CH=CH$_2$) (**6**)

W(1)−O(1)	1.714(6)	W(1)−N(11)	2.167(6)
W(1)−O(2)	1.724(6)	W(1)−N(21)	2.304(6)
W(1)−C(1)	2.135(8)	W(1)−N(31)	2.313(6)
C(1)−C(2)	1.304(13)		
O(1)−W(1)−O(2)	104.2(3)	O(2)−W(1)−C(1)	97.1(3)
O(1)−W(1)−C(1)	96.2(3)	O(2)−W(1)−N(11)	98.4(3)
O(1)−W(1)−N(11)	98.7(3))	O(2)−W(1)−N(21)	167.5(3)
O(1)−W(1)−N(21)	88.3(3))	O(2)−W(1)−N(31)	87.79(25)
O(1)−W(1)−N(31)	168.03(25)	C(1)−W(1)−N(11)	155.1(3)
W(1)−C(1)−C(2)	131.0(7)	C(1)−W(1)−N(21)	82.4(3)
		C(1)−W(1)−N(31)	82.5(3)

signal displayed a trans $^3J_{WH}$ of 19.3 Hz. A broad resonance at 2.52 ppm in the ^{1}H NMR spectrum is assigned to the methyl group of the rotating vinyl fragment. Upon warming to 60 °C, the vinylic methyl group became a sharp singlet at 2.74 ppm. Although the C_β signal is obscured by the aromatic signals of the toluene-d_8 solvent, the C_α signal is found at 190.6 ppm in the ^{13}C{^{1}H} NMR spectrum and is observed as a broad signal with an identical chemical shift in the proton-coupled ^{13}C NMR spectrum. The absence of a large $^1J_{CH}$ for the C_α carbon indicates that the methyl group of the vinyl fragment is attached to C_α. We conclude that the vinyl formation is regioselective with the hydride adding to the terminal alkyne carbon.

X-ray Structure of Tp′W(O)$_2$(CH=CH$_2$) (6). An ORTEP diagram of **6** is shown in Figure 3. Selected bond distances and angles are given in Table 2. Complex **6** adds to the series of Tp′W(O)$_2$(X) complexes that have been structurally characterized (X = Et, Ph,[41,42] SePh,[43] or (μ-O)[Tp′W(O)$_2$][44]). The W−N bond lengths are 2.167(6), 2.304(6), and 2.313(6) Å, clearly demonstrating the greater trans influence of the two oxo units compared to that of the vinyl fragment. The W−O(1) and W−O(2) distances are equal within experimental error. The O(1)−W−O(2) angle of 104.2° and the C(1)−W(1)−N(11) angle of 155.1° are typical of octahedral *cis*-dioxo complexes.[44,45] The N(11)−W−N(21) and N(11)−W−N(31) angles of 78.21° and 78.69° are slightly smaller than the N(21)−W−N(31) angle of 79.71° because of splaying of the two pyrazole ligands about the bisecting vinyl fragment. The vinyl fragment has a W−C(1)−C(2) angle of 131.0°, a W−C(1) distance of 2.135(8) Å, and a C(1)−C(2) length of 1.304(13) Å.

Synthesis and Characterization of Tp′W(O)(OH)(HC≡CH) (9) and Tp′W(O)(OH)(MeC≡CMe) (10). Acetylene resonances and unique shifts for the pyrazole proton and methyl signals suggested that the chiral complex Tp′W(O)(OH)(HC≡CH) (**9**), an isomer of Tp′W(O)$_2$(CH=CH$_2$), might be the minor product obtained from the Al$_2$O$_3$ column that produced the dioxo−vinyl compound. This oxo−hydroxy complex could form via simple deprotonation of the water complex **1** by Al$_2$O$_3$. To support this hypothesis, [Tp′W(O)(H$_2$O)(HC≡CH)][OTf] was dissolved in CH$_2$Cl$_2$ and treated with an excess of aqueous NaOH (eq 6). After stirring the sample for 2 h, filtration through

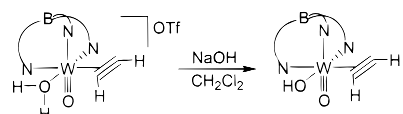

(**9**) (6)

Celite, and removal of solvent, the ^{1}H NMR spectrum of the residue revealed resonances identical to those observed for the minor product **9** acquired from the chromatographic workup of mixtures containing **1** and **3**. The rearrangement of **9** to **6**, which can be considered as the net oxidative addition of the O−H bond across the W−(HC≡CH) fragment, can also be achieved thermally. Heating a C$_6$D$_5$Br sample of **9** at 100 °C resulted in complete conversion to **6** after 48 h.

The ^{1}H NMR of hydroxo−alkyne complex **9** displays acetylene resonances at 11.30 and 10.65 ppm with $^2J_{WH}$ values of 12 and 16 Hz, respectively. Inequivalent coupling to the alkyne is also observed in the ^{13}C NMR spectrum, where the acetylene carbons resonate at 169.7 and 157.8 ppm and possess $^1J_{WC}$ values of 39 and 26 Hz, respectively. The 2-butyne−hydroxo complex, Tp′W(O)(OH)(MeC≡CMe) (**10**), which was prepared by a route identical to the synthesis of **9**, also has differing values for $^1J_{WC}$ (36 and 25 Hz). These data differ from the ^{13}C NMR spectra obtained for Tp′W(O)(HC≡CH)(I) and Tp′W(O)(MeC≡CMe)(I),[33] where the $^1J_{WC}$ values were identical for each alkyne carbon (30 Hz for both complexes), and for [Tp′W(O)(H$_2$O)(HC≡CH)][OTf] (**1**), where $^1J_{WC}$ values are nearly identical (28 and 30 Hz). In addition the $^2J_{WH}$ values for each acetylene proton are identical in Tp′W(O)(HC≡CH)(I) (13 Hz) and [Tp′W(O)(H$_2$O)(HC≡CH)][OTf] (15 Hz). The 13 Hz difference in $^1J_{WC}$ for **9**, the 4 Hz difference in $^2J_{WH}$ values for **9**, and the 11 Hz difference in $^1J_{WC}$ for **10** for the alkyne signals reflect a change in the electronic structure for these hydroxo−alkyne complexes compared to the other oxo−alkyne complexes reported here.

The W(O)(OH)(RC≡CR) fragment is unique in that all three ligands can serve as effective π-electron donors. Scheme 3 shows two different modes of π-electron donation for the OH ligand. Bonding considerations for the M−OR fragment have been reviewed.[46] In case A, the O−H bond is oriented perpendicular to the W−O vector, resulting in donation from the OH oxygen p orbital to the tungsten d_{xz} orbital to form a

(41) Eagle, A. A.; Tiekink, E. R. T.; Young, C. G. *J. Chem. Soc., Chem. Commun.* **1991**, 1746.
(42) Eagle, A. A.; Young, C. G.; Tiekink, E. R. T. *Organometallics* **1992**, *11*, 2934.
(43) Eagle, A. A.; Tiekink, E. R. T.; Young, C. G. *Inorg. Chem.* **1997**, *36*, 6315.
(44) Eagle, A. A.; George, G. N.; Tiekink, E. R. T.; Young, C. G. *Inorg. Chem.* **1997**, *36*, 472.
(45) Brower, D. C.; Templeton, J. L.; Mingos, D. M. P. *J. Am. Chem. Soc.* **1987**, *109*, 5203.
(46) Caulton, K. G. *New. J. Chem.* **1994**, *18*, 25.

Scheme 3. Orientations of Hydroxo O−H Bond

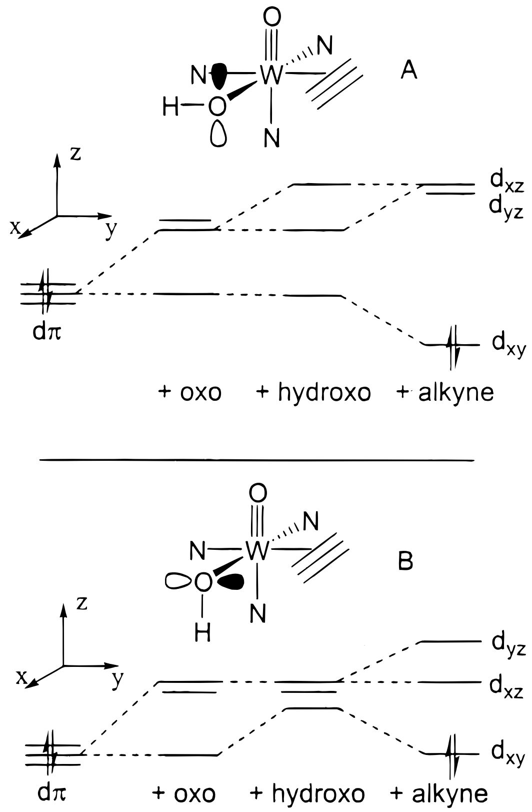

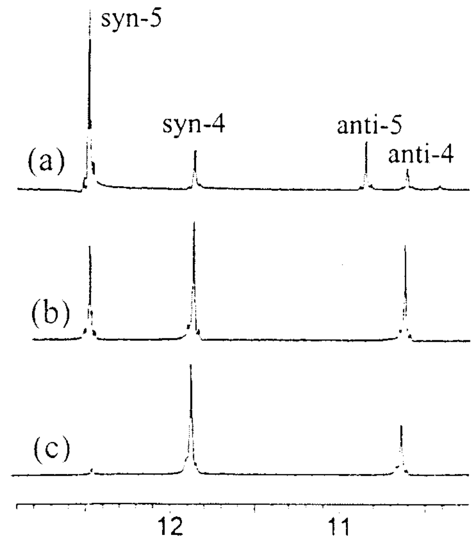

Figure 4. ^{1}H NMR of acetylene region during aqua−propyne formation.

three-center−four-electron bond among oxo, hydroxo, and tungsten. Arrangement B shows parallel O−H and W−O bonds, which create an unfavorable filled−filled interaction between the hydroxo oxygen p orbital and the d_{xy} orbital. Clearly, the perpendicular W═O, O−H relationship of case A would be preferred. For the complexes Tp′W(O)(X)(RC≡CR) (X = I, H_2O, OTf), the alkyne is approximately coplanar with two ligands that do not participate in π bonding: X and a pyrazolyl nitrogen. In the hydroxo complexes, the alkyne should be nearly parallel with the HO−W−N vector such that one end of the alkyne is syn to the π innocent pyrazolyl nitrogen, while the other alkyne C−H unit lies near the π-basic hydroxo group. This disparity in the M−L dπ bonding for the two ligands, which lie along the alkyne axis, may explain the observed difference in alkyne $^1J_{WC}$ and $^2J_{WH}$ values.

Although distinct pyrazole and alkyne signals are observed for **9** and **10**, indicating that proton exchange between the terminal oxo and hydroxo ligands is slow,[47−49] two of the three pyrazole proton signals and four of the six Tp′ methyl signals do broaden when excess water is present as was the case for **1**. This broadening also occurs when solid samples of **9** or **10** are exposed to air for short time periods (<1 h) prior to NMR observation, indicating that the hydroxo complexes are hygroscopic. When a fresh NMR sample of either of the hydroxide complexes is prepared, the hydroxide proton is observed as a very broad singlet near 5.7 ppm for **9** or 4.8 ppm for **10**. As further evidence for the hygroscopic nature of **9** and **10**, the experimentally determined elemental analyses for both complexes consistently showed that an additional water molecule was associated with the hydroxo complexes.

Alkyne Isomerization. To probe the possibility of alkyne rotation during the halide abstraction procedure, iodide substitution products were synthesized from the syn and anti isomers of Tp′W(O)(I)(MeC≡CH) in separate experiments. The syn isomer has the propyne methyl group aligned along the W−N axis directed toward an N atom, while the anti isomer has the propyne methyl group aligned along the W−I axis directed toward the I atom. Addition of AgOTf to the propyne complex *syn*-Tp′W(O)(I)(MeC≡CH) in CH_2Cl_2 resulted in a mixture of neutral triflate−alkyne rotamers **5** and cationic water−alkyne rotamers **4** as assessed by ^{1}H NMR following workup (Scheme 4). The water complexes are generated from adventitious water. Nearly identical product ratios are observed when *anti*-Tp′W(O)(I)(MeC≡CH) is used as starting material in place of *syn*-Tp′W(O)(I)(MeC≡CH). In both cases the ratio between the total syn species (*syn*-**5** + *syn*-**4**) and the total anti species (*anti*-**5** + *anti*-**4**) was 3.36:1. The relative amounts of each complex in the CD_2Cl_2 sample remained unchanged after 6 h at room temperature. A small excess of water was then added to the NMR sample to promote conversion of the triflate adducts, **5**, to the aqua species, **4**. After an additional 6 h, triflate adducts, syn-**5** and anti-**5**, were no longer detectable by ^{1}H NMR and the two aqua isomers, syn-**4** and anti-**4**, were present in a 3.35:1 ratio. Apparently, syn-**5** converts to syn-**4** while anti-**5** forms anti-**4**. The spectra shown in Figure 4 display the changes in the terminal acetylene region during the conversion of **5** to **4** after the addition of water.

Given that the total syn to anti ratio does not change during conversion of the coordinated triflate species to the coordinated water complexes, it appears that the alkyne remains fixed throughout substitution of triflate by water. Since both syn and anti products form from each isomer of Tp′W(O)(I)(MeC≡CH), it then follows that the alkyne isomerization process occurs during formation of the coordinated water or triflate complexes from the iodide precursor complexes. Assuming iodide removal as the initial step, Scheme 5 shows two possible structures, differing in alkyne orientation, for the putative five-coordinate intermediate differing in alkyne orientation. For each case, the modes of addition leading to syn and anti products are presented. Intermediate **A** could account for the greater than 3 to 1 preference for formation of syn versus anti products, since the methyl group, being larger than the acetylene hydrogen, will inhibit approach of L (L = OTf^- or H_2O) along the pathway

(47) Brown, S. N.; Myers, A. W.; Fulton, J. R.; Mayer, J. M. *Organometallics* **1998**, *17*, 3364.
(48) Erikson, T. K. G.; Mayer, J. M. *Angew. Chem., Int. Ed. Engl.* **1988**, *27*, 1527.
(49) Coe, B. J. *Polyhedron* **1992**, *11*, 1085.

Scheme 4. Formation of Aqua−Propyne Rotamers

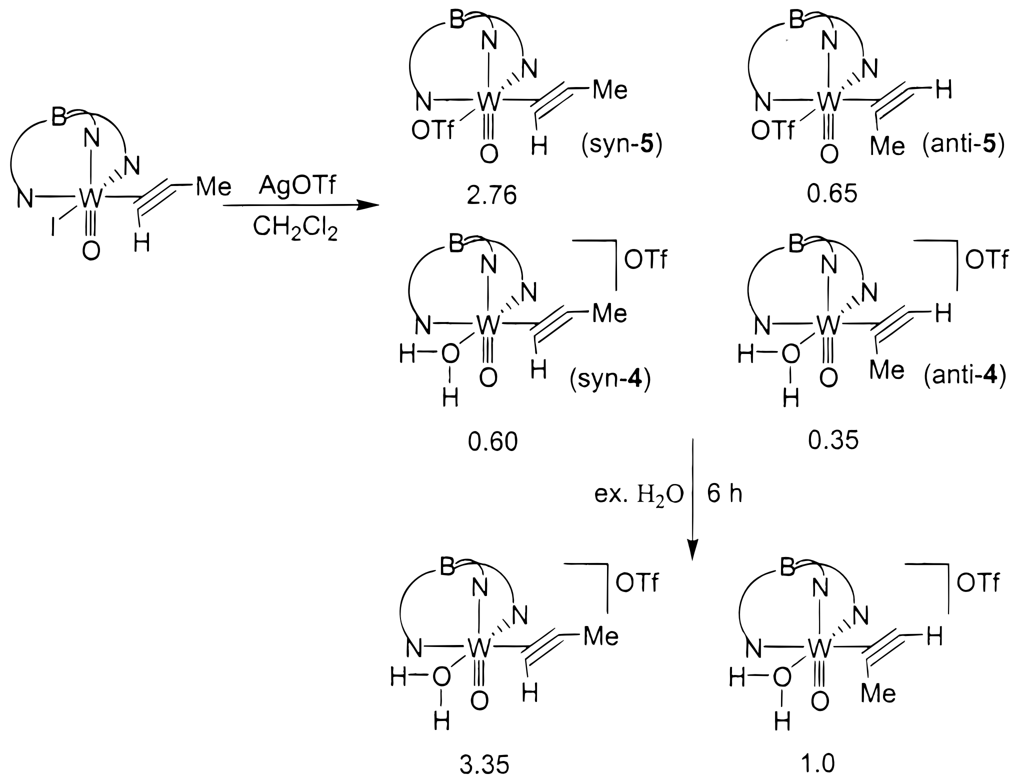

leading to anti product formation. The second possible structure for the five-coordinate intermediate (**B**), surely less attractive electronically, has the C≡C axis aligned parallel to the W═O vector. In this symmetrical intermediate, addition from either side of the mirror plane is equally probable, and then the alkyne would need to rotate 90° to form the product. Rotation such that the propyne methyl group turns away from the incoming group (L = H_2O or OTf^-) would presumably be favored relative to rotation of the methyl group toward L, consistent with the proportion of syn complex observed. However, the parallel relationship between W═O and C≡C present in **B** is energetically disfavored relative to orthogonal W═O and C≡C fragments by as much as 25 kcal/mol in octahedral oxo−alkyne complexes. To our knowledge, all of the known monomeric oxo−alkyne compounds, including Tp′W(O)(RC≡CR)(I),[33] [Re(O)(RC≡CR)$_2$(L)][SbF$_6$] (L = pyridine),[36] and Re(RC≡CR)$_2$(O)Na,[37] approximate a perpendicular arrangement between the M═O and C≡C vectors and do not exhibit fluxional behavior attributable to alkyne isomerization. Structure **A** is the more probable intermediate.

Dynamic Behavior of Water and Hydroxo Complexes. The room temperature ^{1}H NMR spectrum of **1** with added water features broad Tp′ resonances that sharpen as the temperature is lowered. In contrast, the acetylene proton signal near 11.8 ppm was sharp at room temperature and broad at lower temperatures (see Figure 5).

The dynamic behavior in the acetylene region reflects a rapid equilibrium between the aqua complex **1** and the hydroxo species **9** that forms upon deprotonation of the coordinated water of **1** by free water (eq 7). The room temperature ^{1}H NMR spectrum displays signals representing the average of species **1** and **9** in rapid equilibrium. As the NMR probe is cooled, the rate of proton transfer responsible for the equilibrium is decreased. Only the downfield acetylene signal becomes broad, since the difference in chemical shift between **1** and **9** for this acetylene resonance is 0.7 ppm while the chemical shift difference for the further upfield acetylene signals (only 0.02 ppm) and for the remaining Tp′ signals is much smaller. On the basis of the line broadening evident for the downfield acetylene proton at low temperature and the corresponding chemical shift difference for the two complexes, each measured independently, a $\Delta G^{\ddagger}_{293K}$ value of 9.9 kcal mol^{-1} is calculated for this *inter*molecular proton-transfer process. When this equilibrium exchange process is initiated by the addition of excess D_2O to complex **1**, the downfield acetylene signal broadens at a slightly faster rate than with H_2O addition. A

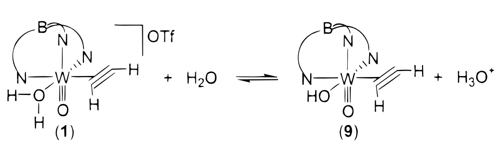

(7)

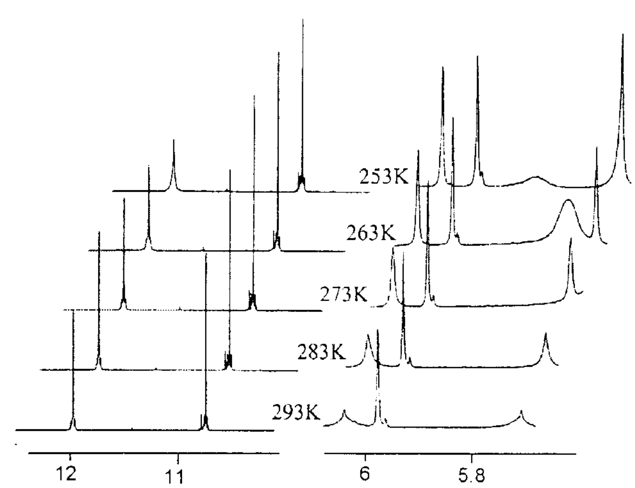

Figure 5. Variable temperature ^{1}H NMR of acetylene (left) and Tp′ methine regions (right) of **1** in the presence of excess water. The broad signal in the Tp′ region at 263 and 253 K is assigned in H_2O.

Scheme 5. Possible Intermediates for Aqua−Propyne Formation

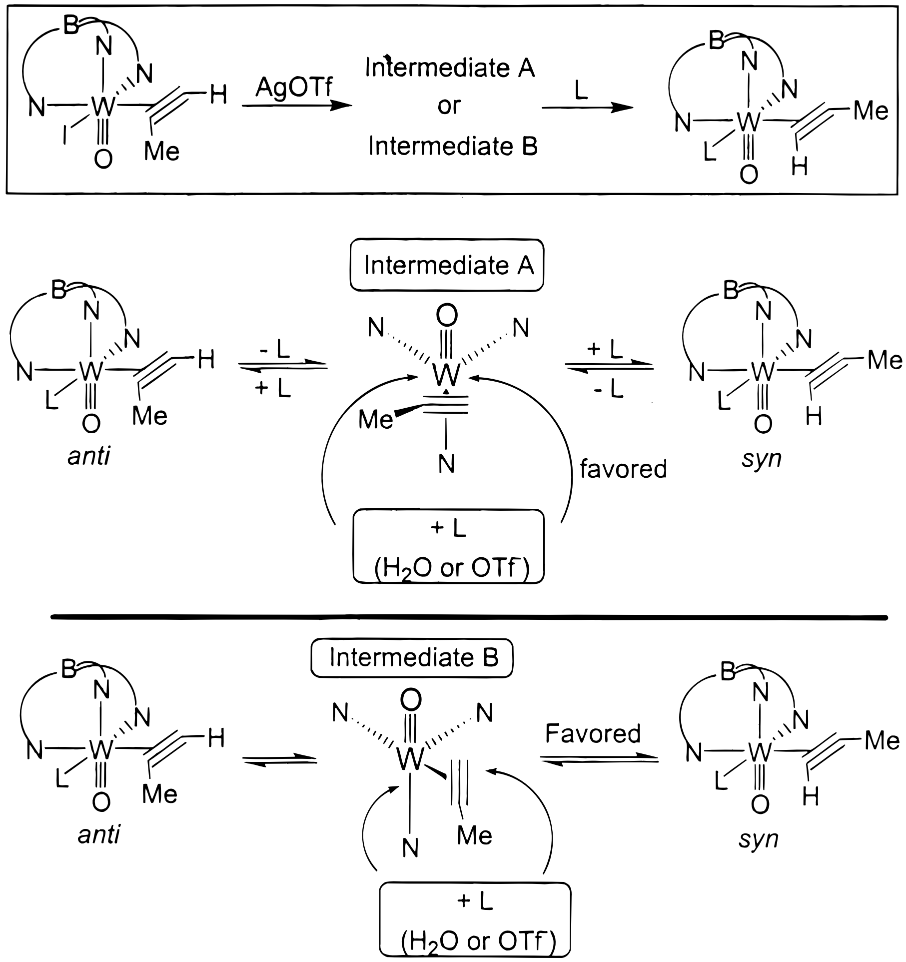

modest k_H/k_D value of 1.2 (±0.1) between 253 and 273 K is obtained, consistent with proton exchange.

Given that the methine resonances (shown in Figure 5) and methyl signals of Tp′ display variable temperature behavior that differs dramatically from that of the acetylene fragment, it is evident that a second fluxional process is occurring. The ^{1}H NMR data indicate that a mirror plane of symmetry is created during this second fluxional process. Furthermore, the ^{1}H NMR spectra indicate that the two ends of the acetylene unit are *not* equilibrating at the observed temperatures. We attribute this higher energy dynamic process to proton exchange between the two coordinated oxygen atoms. This higher energy dynamic process was slower in the presence of an excess of D_2O, giving a k_H/k_D value of 1.7 (±0.1) between 253 and 273 K.

Two possible pathways, both involving the presence of an equilibrium between the aqua and hydroxo complexes, for this second process are shown in Scheme 6. The dihydroxo intermediate [Tp′W(OH)$_2$(HC≡CH)]$^+$ would form upon protonation of the terminal oxo ligand, while the anion [Tp′W(O)$_2$(HC≡CH)]$^-$ would form by deprotonation of the hydroxo ligand. When an NMR sample of of the hydroxo−oxo complex **9** is treated with an equivalent of triethylamine, the ^{1}H NMR spectrum displayed broad Tp′ signals similar to those observed when excess water was added to the aqua complex **1**. Addition of a second equivalent of NEt_3 resulted in coalescence of two of the three Tp′ methine resonances, indicating that the rate of the dynamic process was increased. Conversely, decoalescence of the methine signals, due to a decrease in the rate of the

Scheme 6. Production of Intermediates with C_s Symmetry

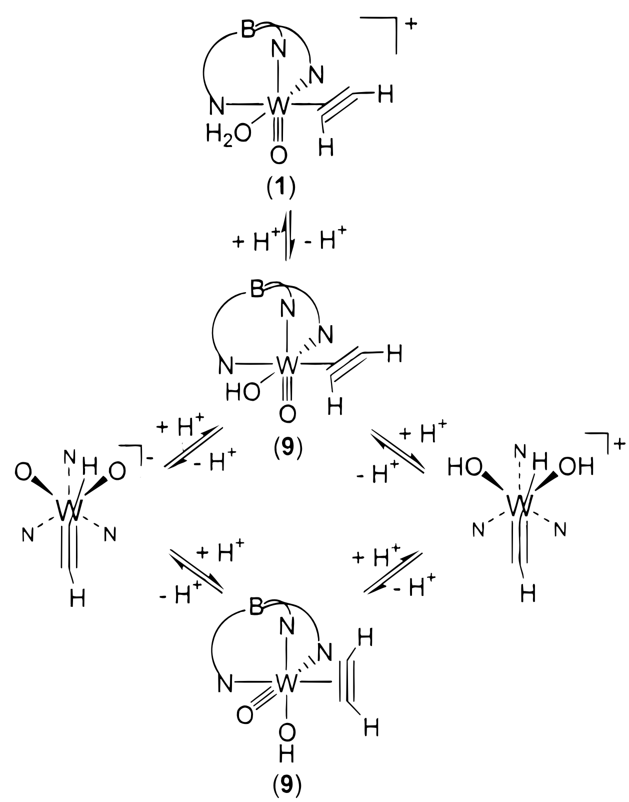

Scheme 7. dπ Orbital Interactions Involved with WO_2 Fragment

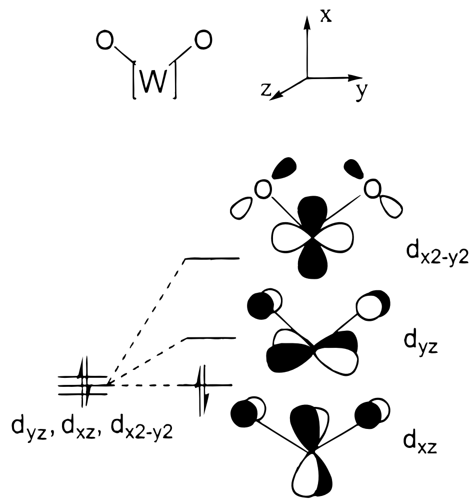

dynamic process, was observed when 2 equiv of HCl was added to this same NMR sample. The downfield acetylene proton appeared near 11.8 ppm in the ^{1}H NMR, indicating that aqua complex **1** was the predominant species present in the equilibrium mixture. These qualitative experiments suggest that the dioxo anion is the symmetrical intermediate involved in the higher energy dynamic process. Another potential mechanism for generating a symmetric intermediate is via simple intramolecular proton transfer from the hydroxo ligand to the adjacent oxo ligand. Since added triethylamine increases the rate of formation of the mirror plane species, we will exclude this intramolecular process from further consideration.

For either the dioxo or dihydroxo intermediates, the alkyne axis would be required to lie on the mirror plane so that the two ends of the acetylene remain distinct. On the basis of the observed line broadening of the Tp′ methine protons, this fluxional process has a $\Delta G^{\ddagger}_{263K}$ value of 14.5 kcal mol^{-1}, well above the activation energy for the low-temperature fluxional process.

A subtle electronic rationale favoring an alkyne orientation on the mirror plane of symmetry can be made. Given that the O–W–O angle should be greater than 90° in either intermediate, the d_{yz} orbital would overlap more with the oxygen π donor p orbitals than the d_{yz}, and hence, it would be raised in energy above the lower energy-filled d_{xz} orbital (Scheme 7). Note that $d_{x^2-y^2}$ is well above both of these dπ levels because of overlap with both oxygen donors. A vertical orientation of the alkyne would then allow back-donation from the filled d_{xz} orbital to the vacant alkyne $\pi_{||}$*. Furthermore, in the alternative horizontal alkyne orientation, the two ends of the acetylene would encounter two methyl groups of the Tp′ ligand in unfavorable steric interactions. Note that the tridentate nature of the Tp′ ligand projects the 3-methyl substituents toward the quadrants lying between adjacent N and O donor atoms rather than along the W–N axes.

Conclusion

Chemistry of the oxo–alkyne fragment [Tp′W(O)(RC≡CR)] has been extended to include cationic aqua complexes. The crystal structure of [Tp′W(O)(H_2O)(MeC≡CMe)][OTf] shows that the complex exists in the solid state with two triflate molecules serving as bridging units between two of the complex cations. The aqua–alkyne complexes, [Tp′W(O)(H_2O)(RC≡CR)][OTf] (R = H or Me), undergo a deprotonation, isomerization sequence, which is promoted by Al_2O_3 to form the W(VI) dioxo–vinyl species Tp′W(O)$_2$(CR=CHR). This isomerization was also shown to occur thermally from Tp′W(O)(OH)(HC≡CH). The putative intermediate Tp′W(O)(OH)(RC≡CR) can be isolated via deprotonation of the aqua–alkyne compound with aqueous NaOH in each case. Formal oxidative addition of the hydroxyl O–H bond across the tungsten–alkyne fragment would then generate the W(VI) dioxo–vinyl complex.

Experimental Section

Materials and Methods. Reactions were performed under a dry nitrogen atmosphere using standard Schlenk techniques. Methylene chloride and pentanes were purified by passage through an activated alumina column under a dry argon atmosphere. Deuterated methylene chloride was deoxygenated using standard freeze–pump–thaw techniques and stored under a nitrogen atmosphere over 4 Å molecular sieves. Distilled water was degassed for several minutes with nitrogen prior to use.

The syntheses of Tp′W(O)(I)(HC≡CH), Tp′W(O)(I)(MeC≡CH), and Tp′W(O)(I)(MeC≡CMe) have been previously reported.[33] Silver trifluoromethanesulfonate (AgOTf) was obtained from Acros Organics. Alumina used for adsorption chromatography (Al_2O_3, 80–200 mesh) was obtained from Fisher Scientific and used directly. Sodium hydroxide was used as a 50 wt % aqueous solution.

^{1}H NMR and ^{13}C NMR spectra were recorded using Bruker NMR spectrometers operating at 400 or 500 MHz for the ^{1}H probe and 100 MHz for the ^{13}C experiments. Infrared spectra were recorded on an ASI Applied System ReactIR 1000 FT-IR spectrometer. Chemical analyses were performed by Atlantic Microlabs of Norcross, GA.

[Tp′W(O)(H_2O)(HC≡CH)][OTf] (1). In a 200 mL round-bottom flask, Tp′W(O)(I)(HC≡CH) (0.123 g, 0.190 mmol) was dissolved in ca. 35 mL of methylene chloride. To this pale-yellow solution, water (30 μL, 1.67 mmol) was added via a microliter syringe. Solid AgOTf (0.055 g, 0.210 mmol) was then added, and the reaction was stirred for 2.5 h. Filtration through Celite removed the AgI precipitate to yield a pale-yellow solution. The solution was concentrated to about 5 mL and layered with pentanes. The resulting yellow crystals were washed 3 × 3 mL with a cold 1:1 solution of pentanes/CH_2Cl_2 to remove any remaining Tp′W(O)(OTf)(HC≡CH) impurity. Yield: 0.055 g (42%). IR (neat solid): ν(OH) 3000 cm^{-1} (broad), $\nu(SO_3)$ 1293 cm^{-1}, ν(W=O) 960 cm^{-1}. ^{1}H NMR (CD_2Cl_2): δ 12.01, 10.63 (s, $^2J_{WH}$ = 15 Hz, *H*CC*H*), 10.05 (bs, *H*$_2$O), 6.16, 6.06, 5.64 (Tp′C*H*), 2.64, 2.49, 2.42, 2.35, 2.30, 1.85 (Tp′ C*H*$_3$). ^{13}C NMR (CD_2Cl_2): δ 156.8, 148.2 ($^1J_{WC}$ = 28 and 30 Hz, respectively, $^1J_{CH}$ = 225 Hz, H*C*CH), 154.6, 153.8, 152.3, 146.9, 146.5, 144.9 (Tp′*C*CH$_3$), 120.1 (q, $^1J_{CF}$ = 318 Hz, O$_3$S*C*F$_3$), 109.3, 108.7, 107.8 (Tp′*C*H), 16.4, 14.2, 14.1, 13.1, 12.7, 12.4 (Tp′*C*H$_3$). Anal. Calcd for $C_{18}H_{26}BF_3N_6O_5SW$: C 31.32; H, 3.80; N, 12.18. Found: C, 31.52; H, 3.74; N, 11.95.

[Tp′W(O)(H_2O)(MeC≡CMe)][OTf] (2). Preparation and crystallization of compound **2** were performed following the procedure for **1**. IR (neat solid): ν(OH) 3100 cm^{-1} (broad), $\nu(SO_3)$ 1299 cm^{-1}, ν(W=O) 946 cm^{-1}. ^{1}H NMR (CD_2Cl_2): δ 10.35 (bs, *H*$_2$O), 6.10, 6.00, 5.64 (s, Tp′C*H*), 3.13, 2.17 (s, C*H*$_3$C≡CC*H*$_3$), 2.46, 2.42, 2.36, 2.26, 2.10, 1.70 (s, Tp′C*H*$_3$). ^{13}C NMR (CD_2Cl_2): δ 167.9, 155.7 ($^1J_{WC}$ = 28 and 27 Hz, respectively, Me*C*≡*C*Me), 152.8, 152.8, 151.9, 146.3, 146.2, 144.1 (Tp′*C*CH$_3$), 119.5 (q, $^1J_{CF}$ = 320 Hz, O$_3$S*C*F3), 108.6, 107.9, 107.3 (Tp′*C*H), 17.3, 17.1, 16.0, 13.9, 13.3, 13.1, 12.5, 12.2 (6 Tp′C*C*H$_3$ and *C*H$_3$C≡C*C*H$_3$). Anal. Calcd for $C_{20}H_{30}N_6BF_3O_5SW$: C, 33.45; H, 4.21; N, 11.71. Found: C, 33.48; H, 4.32; N, 11.68.

Tp′W(O)(OTf)(HC≡CH) (3). In a 200 mL round-bottom flask, Tp′W(O)(I)(HC≡CH) (0.136 g, 0.210 mmol) was dissolved in ca. 35 mL of methylene chloride. While the sample was being stirred, AgOTf (0.065 g, 0.253 mmol) was added. Precipitation of AgI was observed within minutes following addition, and the reaction was allowed to stir for 2 h at room temperature. Filtration through Celite removed the AgI precipitate to afford a pale-yellow solution. The solvent was removed in vacuo leaving a gray-yellow solid. Yield: 0.120 g (86%). A small amount of **1** (5–10% by ^{1}H NMR) is consistently formed during this synthesis. IR (neat solid): $\nu(SO_3)$ 1335 cm^{-1}, ν(W═O) 986 cm^{-1}. ^{1}H NMR (CD_2Cl_2): δ 12.47, 10.71 (s, $^2J_{WH}$ = 15 Hz, *H*CC*H*), 6.17, 6.05, 5.65 (s, Tp′C*H*), 2.64, 2.49, 2.42, 2.35, 2.32, 1.91 (s, Tp′C*H*$_3$). ^{13}C NMR (CD_2Cl_2): δ 156.5, 148.6 ($^1J_{WC}$ = 29 Hz, H*CC*H), 154.4, 153.5, 152.8, 146.8, 145.8, 145.1 (Tp′*C*CH$_3$), 119.3 (q, $^1J_{CF}$ = 318 Hz, O$_3$S*C*F$_3$), 109.3, 108.3, 107.7 (Tp′*C*H), 16.4, 14.3, 14.0, 13.1, 12.7, 12.5 (Tp′*C*H$_3$). Because of contamination with **1**, satisfactory elemental analysis of this hygroscopic solid was not obtained.

[Tp′W(O)(H$_2$O)(MeC≡CH)][OTf] (4). Preparation of compound **4** was performed following the procedure for **1**. Compound **4** was isolated as a 4 to 1 mixture of alkyne rotamers. IR (neat solid): ν(OH) 3100 cm^{-1} (broad), $\nu(SO_3)$ 1295 cm^{-1}, ν(W═O) 953 cm^{-1}. ^{1}H NMR (major isomer, CD_2Cl_2): δ 11.95 (q, $^2J_{WH}$ = 15 Hz, $^4J_{HH}$ = 2.5 Hz, *H*CCMe), 9.92 (bs, *H*$_2$O), 6.15, 6.04, 5.67 (s, Tp′C*H*), 2.50, 2.37, 2.36, 2.32, 2.23, 1.85 (Tp′C*H*$_3$), 2.34 (d, $^4J_{HH}$ = 2.5 Hz, C*H*$_3$CCH). ^{1}H NMR (minor isomer, CD_2Cl_2): δ 10.60 (q, $^2J_{WH}$ = 15 Hz, $^4J_{HH}$ = 2.5 Hz, *H*CCMe), 9.46 (bs, *H*$_2$O), Tp′C*H* signals overlap with major isomer, 3.38 (d, $^4J_{HH}$ = 2.5 Hz, C*H*$_3$CCH), 2.63, 2.44, 2.43, 2.08 (Tp′C*H*$_3$, remaining Tp′ signals overlap with major isomer). ^{13}C NMR (major isomer, CD_2Cl_2): δ 169.1, 157.1 ($^1J_{WC}$ = 28 Hz, H*C*≡*C*Me), 153.0, 152.9, 151.1, 146.4, 146.3, 144.2 (Tp′*C*CH$_3$), 119.5 (q, $^1J_{CF}$ = 320 Hz, O$_3$S*C*F3), 108.7, 108.0, 107.3 (Tp′*C*H), 17.3, 14.0, 13.8, 13.3, 13.0, 12.6, 12.3 (6 Tp′C*C*H$_3$ and *H*C≡C*C*H$_3$). Anal. Calcd for $C_{19}H_{28}N_6BF_3O_5SW\cdot H_2O$: C, 32.40; H, 4.01; N, 11.94. Found: C, 31.60; H, 4.19; N, 11.64.

Tp′W(O)$_2$(CH═CH$_2$) (6). A column was prepared with dry hexanes and 100 mL of Al_2O_3. The column was loaded with **1** (0.630 g, 0.913 mmol) and eluted with CH_2Cl_2. The column was monitored by thin-layer chromatography, and a single colorless fraction was collected. Removal of solvent and recrystallization from CH_2Cl_2/pentanes produced colorless crystals. Yield: 0.33 g (67%). IR (neat solid): ν(W═O) 945, 905 cm^{-1}. ^{1}H NMR (CD_2Cl_2): δ 7.46 (dd, $^3J_{HH}$ = 19.2 Hz, $^3J_{HH}$ = 13.6 Hz, $^2J_{WH}$ = 4.8 Hz, C*H*$_\alpha$ = CH$_2$), 6.98 (dd, $^3J_{HH}$ = 13.6 Hz, $^2J_{HH}$ = 3.2 Hz, $^3J_{WH}$ = 16.0 Hz, CH═C*H*$_2$ cis to H$_\alpha$), 6.14 (dd, $^3J_{HH}$ = 19.2 Hz, $^2J_{HH}$ = 3.2 Hz, $^3J_{WH}$ = 8.7 Hz, CH═C*H*$_2$ trans to H$_\alpha$), 5.95, 5.88 (1:2 Tp′C*H*), 2.56, 2.54, 2.39, 2.38 (3:6:6:3, Tp′C*H*$_3$). ^{13}C NMR (CD_2Cl_2): δ 177.7 ($^1J_{WC}$ = 151 Hz, $^1J_{CH}$ = 144 Hz, $^2J_{CH}$ = 4 Hz, W−*C*H═CH$_2$), 153.9, 153.8, 148.3, 144.9 (2:1:1:2 Tp′*C*CH$_3$), 135.8 ($^2J_{WC}$ = 29 Hz, $^1J_{CH}$ = 154 Hz, $^2J_{CH}$ = 4 Hz, W−CH═*C*H$_2$), 107.8, 107.7 (1:2 Tp′*C*H), 15.6, 15.2, 12.8, 12.6 (1:2:1:2 Tp′C*C*H$_3$). Anal. Calcd for $C_{17}H_{25}N_6BO_2W\cdot CH_2Cl_2$: C, 37.11; H, 4.50; N, 14.43. Found: C, 37.11; H, 4.71; N, 14.50.

Tp′W(O)$_2$[C(Me)═C(H)(Me)] (7). This complex was synthesized from **2** following the procedure for **6**. IR (neat solid): ν(W═O) 909 and 933 cm^{-1}. ^{1}H NMR (CD_2Cl_2, −50 °C, two isomers in a 10:1 ratio): δ major 5.93, 5.82 (1:2 Tp′C*H*), 5.10 (q, $^3J_{HH}$ = 6 Hz, CMe═C(*H*)(Me)), 2.58, 2.46, 2.34, 2.34, 2.32 (Tp′C*H*$_3$ and CC*H*$_3$═C(H)(Me)), 1.28 (d, $^3J_{HH}$ = 6 Hz, CMe═(H)(C*H*$_3$)); δ minor 6.74 (q, $^3J_{HH}$ = 6 Hz, CMe═C(Me)(*H*)), Tp′*H* and Tp′C*H*$_3$ overlap with Tp′ signals of the major isomer, 1.55 (d, $^3J_{HH}$ = 6 Hz, CMe═C(H)(*Me*)). ^{13}C NMR (CD_2Cl_2): δ major 183.1 ($^1J_{WC}$ = 147 Hz, W−*C*Me═C(H)(Me)), 153.1, 152.6, 147.4, 144.1 (2:1:1:2, Tp′*C*CH$_3$), 136.6 (W−CMe═*C*(H)(Me)), 106.9, 106.7 (1:2, Tp′*C*H), 29.7, 15.3, 15.2, 14.4, 12.6, 12.3 (W−C(*C*H$_3$)═C(H)(*C*H$_3$) and Tp′*C*H$_3$); δ minor 172.4 (W−*C*Me═C(H)(Me)), 152.7, 152.6, 147.7, 144.2 (1:2:1:2, Tp′*C*CH$_3$), 142.8 (W−CMe═*C*(H)(Me)), 20.1, 16.0, 14.3, 12.6 (Tp′*C*H$_3$ and W−C(*C*H$_3$)═C(*C*H$_3$)(H), other signals overlap with major isomer. Anal. Calcd for $C_{19}H_{29}BN_6O_2W$: C, 40.17; H, 5.15; N, 14.78. Found: C, 40.35; H, 5.21; N, 14.76.

Tp′W(O)$_2$(CMe═CH$_2$) (8). This complex was synthesized from **4** following the procedure for **6**. IR (neat solid): ν(W═O) 908 and 940 cm^{-1}. ^{1}H NMR (CD_2Cl_2): δ 6.24 (bs, $^3J_{WH}$ = 19.3 Hz, CMe═C*H*H trans to W), 5.92, 5.86 (s, 1:2, Tp′C*H*), 4.71 (bs, CMe═CH*H* cis to W), 2.54, 2.47, 2.40, 2.38 (s, 3:6:6:3, Tp′CC*H*$_3$), 2.52 (bs, W−C(C*H*$_3$)═CH$_2$. ^{13}C NMR (60 °C, toluene-*d*$_8$): δ 190.6 (W−*C*Me═CH$_2$), 154.8, 154.0, 146.7, 143.8 (2:1:1:2, Tp′*C*CH$_3$), 107.8, 107.5 (2:1, Tp′*C*H), 15.4, 15.3, 12.3, 12.2 (1:2:1:2, Tp′*C*H$_3$), 1.38 (W−C(*C*H$_3$)═CH$_2$).

Tp′W(O)(OH)(HC≡CH) (9). In a 200 mL round-bottom flask, 120.0 mg (0.174 mmol) of **1** was dissolved in 30 mL of CH_2Cl_2. An excess (ca. 10-fold) of NaOH (50 wt % aqueous solution) was added, and the reaction was stirred for 3 h. The solution was concentrated to a volume of ca. 15 mL, and the remaining solution was filtered through Celite to remove any undissolved particles. Removal of solvent afforded the product as a white solid. Yield: 0.060 mg (64%). IR (neat solid): ν(W═O) 945 cm^{-1}. ^{1}H NMR (CD_2Cl_2): δ 11.30, 10.65 ($^2J_{WH}$ = 12.4 and 16.2 Hz, respectively, *H*CC*H*), 6.08, 5.97, 5.59 (Tp′C*H*), 5.70 (O*H*), 2.74, 2.47, 2.41, 2.39, 2.30, 1.79 (Tp′ C*H*$_3$). ^{13}C NMR (CD_2Cl_2): δ 169.7, 157.8 ($^1J_{WC}$ = 39 and 26 Hz, respectively, H*CC*H) 153.54, 152.0, 150.3, 145.2, 144.6, 143.6 (Tp′*C*CH$_3$), 108.4, 107.7, 107.1 (Tp′*C*H), 16.0, 14.3, 14.1, 13.0, 12.6, 12.4 (Tp′*C*H$_3$). Anal. Calcd for $C_{18}H_{26}N_6BO_2W\cdot H_2O$: C, 36.70; H, 4.89; N, 15.09. Found: C, 37.10; H, 4.62; N, 14.78.

Tp′W(O)(OH)(MeC≡CMe) (10). Synthesized following the procedure for **7**. IR (neat solid): ν(W═O) 938 cm^{-1}. ^{1}H NMR (CD_2Cl_2): δ 6.03, 5.93, 5.59 (Tp′C*H*), 4.76 (O*H*), 3.01, 2.17 (C*H*$_3$C≡CC*H*$_3$), 2.64, 2.44, 2.37, 2.28, 2.23, 1.68 (Tp′C*H*$_3$). ^{13}C NMR (CD_2Cl_2): δ 174.5, 160.0 ($^1J_{WC}$ = 36 and 25 Hz, respectively), 151.9, 151.0, 149.8, 144.6, 144.5, 142.9 (Tp′*C*CH$_3$), 107.7, 107.1, 106.6 (Tp′*C*H), 17.8, 15.8, 14.7, 13.8, 13.2, 13.0, 12.6, 12.3 (6 Tp′*C*H$_3$ and *C*H$_3$C≡C*C*H$_3$). Anal. Calcd for $C_{19}H_{29}BN_6O_2W\cdot H_2O$: C, 38.94; H, 5.33; N, 14.34. Found: C, 39.04; H, 5.02; N, 14.29.

^{1}H NMR Study of Alkyne Isomerization with Tp′W(O)(OTf)(MeC≡CH) (5) and [Tp′W(O)(H$_2$O)(MeC≡CH)][OTf] (4) Mixture. Starting with a single alkyne rotamer of Tp′W(O)(MeC≡CH)(I), a mixture of **4** and **5** was generated following the synthesis procedure for the preparation of complex **1**. Approximately 0.050 g of the product mixture was placed in an NMR tube and dissolved in ca. 0.7 mL of dry CD_2Cl_2. Four species were observed in the ^{1}H NMR spectra. The two alkyne rotamers of **4** had terminal acetylene signals at 11.94 and 10.61 ppm, each coupled to the propyne methyl group with $^4J_{HH}$ = 2.5 Hz. The two rotamers of **5** had terminal acetylene signals at 12.44 and 10.84 ppm also with $^4J_{HH}$ = 2.5 Hz. The relative amounts of each component were determined by integration of these terminal alkyne resonances. After 2 h, the relative intensities were unchanged. To promote the formation of **4**, 5 μL of H_2O were added to the NMR sample, and complete conversion to the aqua adduct **4** resulted within 6 h. Regardless of which pure propyne rotamer of Tp′W(O)(MeC≡

Table 3. Crystallographic Data Collection Parameters for **2** and **6**

complex	**2**	**6**
formula	$C_{20}H_{30}N_6BO_5SF_3W$	$C_{17}H_{25}N_6BO_2W$
molecular weight, g/mol	720.04	539.43
crystal system	monoclinic	triclinic
space group	$P2_1/n$	P1
a, Å	16.8117(7)	7.9595(7)
b, Å	10.5521(5)	8.6224(8)
c, Å	20.0591(9)	16.4166(15)
α, deg		76.759(2)
β, deg	112.238(1)	76.158(2)
γ, deg		78.260(2)
V, Å^3	3293.8(3))	1051.61(17)
Z	4	2
density calcd, g/cm^3	1.791	1.798
F(000)	1753.64	555.62
crystal dimensions, mm	0.30 × 0.20 × 0.15	0.15 × 0.15 × 0.20
temp, °C	−100	−100
Mo Kα radiation, Å	0.710 73	0.710 73
2θ range, deg	55.0	50.0
μ, mm^{-1}	3.96	5.61
scan mode	omega	omega
total no. of reflections	39400	6180
total no. of unique reflections	7606	3714
no. of obsd data ($I > 2.5\sigma(I)$)	6315	3354
R_F,[a] %	2.3	4.4
R_w,[b] %	2.8	4.8
GOF[c]	1.15	3.31

[a] $R_F = \sum||F_o| - |F_c||/\sum|F_o|$. [b] $R_w = [\sum w(|F_o| - |F_c|)^2/\sum wF_o^2]^{1/2}$. [c] $GOF = [\sum w(|F_o| - |F_c|)^2/(N_{refl} - N_{params})]^{1/2}$.

CH)(I) was used as starting material, the final propyne rotamer ratio of *syn*-**4** to *anti*-**4** was ca. 3.3:1.

X-ray Crystallography. To collect structural data, single crystals of **2** and **6** were mounted on a glass wand and coated with epoxy. Diffraction data were collected on a Siemens SMART diffractometer using the ω-scan mode. The yellow crystal of **2** was monoclinic with a space group of $P2_1/n$. The colorless crystal of **6** was triclinic with a $P\bar{1}$ space group. Complete details are given in Table 3.

Acknowledgment. We gratefully acknowledge the National Science Foundation (Grant CHE-9727500) for support of this research.

Supporting Information Available: X-ray crystallographic files in CIF format for the structure determinations of **2** and **6**. This material is available free of charge via the Internet at http://pubs.acs.org.

IC990994Y